Nonlinear current-voltage characteristics due to quantum tunneling of phase slips in superconducting Nb nanowire networks

M. Trezza, C. Cirillo, P. Sabatino, G. Carapella, S. L. Prischepa, and C. Attanasio
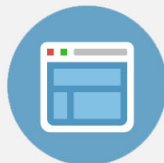
Nonlinear current-voltage characteristics due to quantum tunneling of phase slips in superconducting Nb nanowire networks

M. Trezza,[1] C. Cirillo,[1] P. Sabatino,[1] G. Carapella,[1] S. L. Prischepa,[2] and C. Attanasio[1]

[1]*CNR-SPIN Salerno and Dipartimento di Fisica "E. R. Caianiello", Università degli Studi di Salerno, Fisciano (Sa) I-84084, Italy*

[2]*Belarusian State University of Informatics and Radioelectronics, P. Browka 6, Minsk 220013, Belarus*

We report on the transport properties of an array of $N \sim 30$ interconnected Nb nanowires, grown by sputtering on robust porous Si substrates. The analyzed system exhibits a broad resistive transition in zero magnetic field, H, and highly nonlinear $V(I)$ characteristics as a function of H, which can be both consistently described by quantum tunneling of phase slips. © 2013 AIP Publishing LLC. [http://dx.doi.org/10.1063/1.4851240]

Superconductivity in one-dimensional (1D) nanowires has been object of intensive studies in the last two decades.[1–8] This great interest rose since superconducting nanowires involve fundamental phenomena such as macroscopic quantum tunneling and quantum phase transitions[9–12] and, in addition, they can find applications in classical[13] and possibly quantum information-processing devices,[14,15] or they can be used as interconnects in electronic nanostructured devices.[16] The main point in the study of superconducting nanowires is to understand how their superconducting properties change when the 1D limit is approached. Theoretical studies predicted that the resistance of the wire remains different from zero also at a temperature T well below the critical temperature, T_c, when the wire diameter is smaller than its superconducting coherence length. This effect is related to the presence of both thermal activation and quantum tunneling of phase slips (TAPS and QPS, respectively).[9,11,17] Several experiments have confirmed the presence of QPS phenomena in various superconducting materials and systems.[5,6,12,18,19]

Recently, we developed a nanofabrication approach, which can produce samples with physical properties resembling those of single nanowires.[19] The formation of interconnected networks consisting of ultrathin superconducting Nb nanowires was achieved by using porous silicon (PS) as a template. Due to the extremely reduced Nb thickness, $d_{Nb} \sim 10$ nm, the deposited material tends to occupy only the substrate pitch. As a consequence, the sputtered films, at a later stage patterned into microbridges (length $L_b = 100\,\mu m \times$ width $W_b = 10 - 20\,\mu m$) by standard optical lithography and lift-off procedure, resulted in a network of 250–500 interconnected nanowires, whose average diameter, σ, was comparable to ξ, so that each individual nanowire behaved as a 1D object. The samples exhibited nonzero resistance over a broad temperature range below T_c, and the data were explained considering the occurrence of TAPS and QPS processes. However, no signatures of the presence of QPS phenomena were detected in the current-voltage characteristics, $V(I)$, of the samples.

The experimental results we show in this Letter deal with microbridges [fabricated using Electron Beam Lithography (EBL)] whose in-plane area was 50 times smaller than the previous samples. As a consequence, the resulting network has a drastically lower number of interconnected nanowires ($N \sim 30$). We examine current transport properties of a sample with $d_{Nb} = 12$ nm. As for the data presented in Ref. 19, the $R(T)$ transition curve is satisfactorily reproduced considering the contribution of quantum fluctuations of the superconducting order parameter. In addition, $V(I)$ curves, measured at different magnetic fields, have a behavior typical of 1D superconducting individual nanowires, which is nicely reproduced considering only QPS processes.[1,9]

Porous templates were fabricated by electrochemical anodic etching of n-type, 0.01 Ω cm, monocrystalline Silicon wafers.[20,21] The resulting robust porous substrates, about 2 cm^2 large, have average pore diameter $\O = 15$ nm and average interpore distance $a = 50$ nm. The measured samples were patterned in a four-terminal geometry consisting of a pair of current-carrying Nb electrodes, which contact the ($L_b = 30\,\mu m \times W_b = 1.67\,\mu m$) nanoporous Nb film and a pair of voltage pads 10 μm apart, see Fig. 1(a). This geometry was realized using EBL, performed in a FEI Inspect-F field emission scanning electron microscope (FE-SEM) equipped with a Raith Elphy Plus pattern generator and a lift-off procedure. A 1.5-μm-thick (both to obtain a clean lift-off process and to fully cover the substrate pores) positive tone resist consisting of 9% polymethylmethacrylate (PMMA) 950 K MW dissolved in anisole was spin-coated onto a nanoporous Si substrate and baked at 180 °C on a hotplate for 90 s. The exposition was carried out using a clearance dose of 300 $\mu C/cm^2$ at 30 KV. After exposure, PMMA was developed in a methyl isobutyl ketone and isopropyl alcohol solution (1-MIBK:3-IPA) for 30 s, followed by rinsing in IPA and deionized water. On this mask, Nb ultrathin films were deposited by UHV dc diode magnetron sputtering system with a base pressure in the low 10^{-8} mbar regime following the same fabrication procedure described elsewhere.[20,21] Since the effect of the periodicity of the template tends to disappear when $d_{Nb} \gtrsim \O$,[20] films thicker than 12 nm can hardly be used to obtain a Nb nanowire network. The value $d_{Nb} \sim 12$ nm also assures that individual nanowires are continuous and that the presence of a well defined network is still preserved.[19] The final lift-off procedure in acetone allows to obtain the small-area array of interconnected Nb nanowires shown in Figs. 1(b) and 1(c). As already
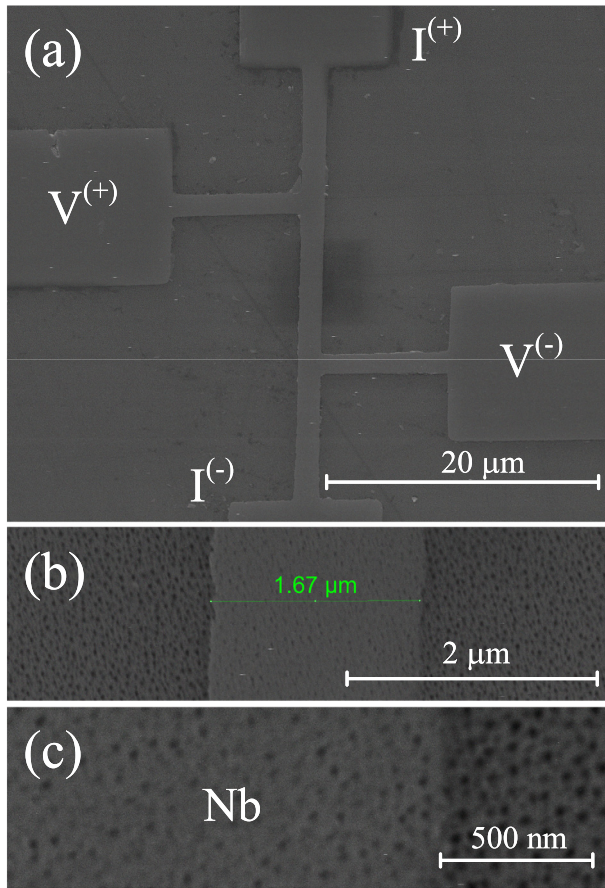
FIG. 1. (a) FE-SEM images of the sample geometry. (b) A middle portion of the Nb film. (c) Zooming-in of the nanoporous Nb film edge.
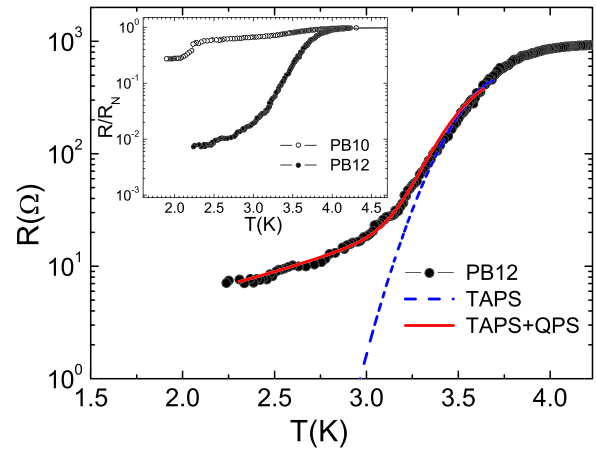

FIG. 2. Zero field transition curve, $R(T)$, of the sample PB12. Points represent the experimental data while the dashed blue (solid red) line is the theoretical curve obtained including only TAPS (both TAPS and QPS) contribution in Eq. (1). The inset shows the $R(T)/R_N$ curves of the samples PB10 and PB12.

underlined, the effect of the patterning is to reduce the number N of interconnected wires under study. From the values of W_b, L_b, a, $\varnothing$, and $w = a - \varnothing$, N can be easily estimated to be around 30. The effective diameter for each wire is $\sigma \sim \sqrt{d_{Nb} \cdot w} \sim 20$ nm.

Current transport measurements were resistively performed in a ^{4}He cryostat using a standard dc four-probe technique. The $V(I)$ characteristics were recorded under current drive condition at different magnetic fields oriented perpendicularly to the plane of the sample. During the measurement, the temperature stabilization was around 1 mK, and in order to minimize any heating effect, the sample was kept in contact with liquid helium. The current biasing was realized by sending rectangular current pulses to the sample, with the current-on time being of 12 ms followed by a current-off time of 1 s. Any single voltage value was acquired at the maximum value of the current. From resistance versus field, $R(H)$, measurements performed at fixed temperature the perpendicular field phase diagram, $H_{c2\perp}(T)$, was obtained, and the zero temperature Ginzburg-Landau coherence length was estimated, $\xi(0) = 10$ nm. For further information on both the normal-state and morphological properties of our samples, the reader can refer to Ref. 19, where the central issue of their homogeneity, which can in principle be responsible of the observed excess of dissipation,[16,22] has been largely discussed.

Fig. 2 shows the $R(T)$ transition curve of the porous Nb bridge with $d_{Nb} = 12$ nm (PB12) measured biasing the sample with a constant current $I_b = 1 \mu$A. The value of the

superconducting critical temperature, $T_c = 3.67$ K, is taken as the temperature at which the resistance R is reduced to half of $R_N = 930 \Omega$, the low-temperature normal-state resistance of the nanowire network. Due to the quasi-1D nature of our samples, their properties are all extremely sensitive to both N and d_{Nb}. To stress this aspect, in the inset of Fig. 2, the resistive curve is reported also for the bridge with $d_{Nb} = 10$ nm (PB10), which does not show any transition to the superconducting state down to $T = 1.8$ K. Moreover, a nanowire network with the same value for d_{Nb}, with a very similar value for w but with $N = 250$ had $T_c = 3.52$ K.[19] The main feature of the $R(T)$ curve of the sample PB12 is the long resistance tail at low temperatures, which can be associated to the occurrence of 1D superconductivity. In particular, following the same approach we used in Ref. 19, the measured temperature dependence of the resistance can be reproduced using[12]

$$R(T) = [R_N^{-1} + (R_{TAPS} + R_{QPS})^{-1}]^{-1}, \quad (1)$$

where R_{TAPS} and R_{QPS} represent the contribution to the resistance due to thermal activation and quantum tunneling of phase slips, respectively. It is $R_{TAPS} \sim \sqrt{F(T)/k_B T} \exp(-F(T)/k_B T)$ (Refs. 17 and 19) and, with exponential accuracy[11,19,22,23]

$$R_{QPS}(T) \approx A \frac{R_Q^2}{R_N} \frac{L^2}{\xi^2(0)} \exp\left[-A \frac{R_Q}{R_N} \frac{L}{\xi(T)}\right], \quad (2)$$

where the quantum resistance $R_Q \approx 6.45$ kΩ, L is the nanowire length and A is a numerical parameter of the order of the unity. $\xi(T) = \xi(0)/\sqrt{1 - T/T_c}$ and $F(T) = F(0)(1 - T/T_c)^{3/2}$ are the temperature dependent coherence length and phase slip activation energy, respectively. The results of the theoretical analysis are reported in Fig. 2 where the best fit curve, which contains T_c, A, and L as adjustable parameters, and nicely reproduces the experimental data, is represented by the solid red line. Interestingly, the fitting procedure gives $T_c = 3.64$ K, a value very close to the measured one, and $A \approx 0.1$ a number which is in good

agreement with the values reported for this parameter in the case of single Ti nanowires.[22] Moreover, the length L of the single nanowire appearing in the expression of R_{QPS} was treated as a fitting parameter.[19] The obtained value, $L \approx 70$ nm, appears to be rather small if directly compared to the estimated length, around $10 \mu m$, of a single continuous nanowire present in the network. This discrepancy could be explained considering that L is not a quantity which can be strictly defined for the network. Moreover, the theoretical models we used were developed for the case of an individual wire and in a disordered network L is more likely a "percolation" length. If, on the other hand, only the TAPS dependence is considered and the QPS term is disregarded in Eq. (1), the obtained curve strongly deviates from the measurements (dashed blue line in Fig. 2).

To further highlight the role played at low temperature by QPS processes, we measured $V(I)$ characteristics as a function of the field[24] at the lowest temperature reached when the resistive transition measurement was recorded. The curves were obtained, in pulse mode, sweeping the current first upward and then downward in presence of several magnetic fields. From the $V(I)$ curves, we have preliminarily estimated the critical current of the single wire, i_c, through the relation $I_c = (N+1)i_c$, where I_c is the critical current of the entire network.[25] i_c is also related to the single wire depairing current, i_{dp}, via $i_c = 2i_{dp}/3\sqrt{3}$.[25] At zero field and $t \simeq 0.6$ we have $I_c = 32 \mu A$, so that $i_c \sim 1 \mu A$. This number is only a factor of two lower than the one obtained at zero field and $t \simeq 0.5$ on the network of 250 nanowires with a similar value of σ where $I_c = 470 \mu A$.[19] As a consequence, also the zero temperature depairing current density[26] of the single wire $j_{dp}(0) = j_{dp}(t)(1-t)^{-1.5} \sim [i_{dp}(t)(1-t)^{-1.5}]/\sigma^2 \simeq 1.9 \times 10^{10} A/m^2$ is comparable to the one reported in the case of the network with $N = 250$ and in the case of perforated Nb films.[19,27] This result indicates that the further reduction of N does not significantly depress the superconducting properties of the single wire and confirms, again, the good quality of the sample ruling out the presence of tunneling barriers at the grain boundaries.[16] In Fig. 3(a), we show the $V(I)$ curve measured at $T = 2.2$ K $(t \equiv T/T_c \simeq 0.6)$ and $\mu_0 H = 0.01$ T. As expected, being the temperature far from T_c, the curve, as can be inferred from the red dotted line, does not show multiple steps corresponding to more and more phase slip lines entering the sample but only one large step is observed.[28] It is also important to notice that, in small applied fields, a clear hysteresis was present, which became weaker when the field was increased, completely disappearing for $\mu_0 H > 0.14$ T. We rule out the heating as possible cause of the hysteresis since, after the phase slip has entered the sample, all the $V(I)$ curves, before reaching the normal state, are linear and they do not extrapolate to zero.[28] In particular, the width of the hysteresis ranged from $\Delta(I) \equiv I_{up}(10 mV) - I_{down}(10 mV) = 1.50 \mu A$ for $\mu_0 H = 0.01$ T to the value $\Delta(I) = 0.40 \mu A$ for $\mu_0 H = 0.14$ T. This behavior is qualitatively similar to what observed in NbSe$_2$ nanowires where the hysteresis vanished as the temperature was raised towards T_c (Ref. 29) though, in our case, this value of the field is considerably far from $\mu_0 H_{c2\perp}(t \simeq 0.6) \sim 1.2$ T.

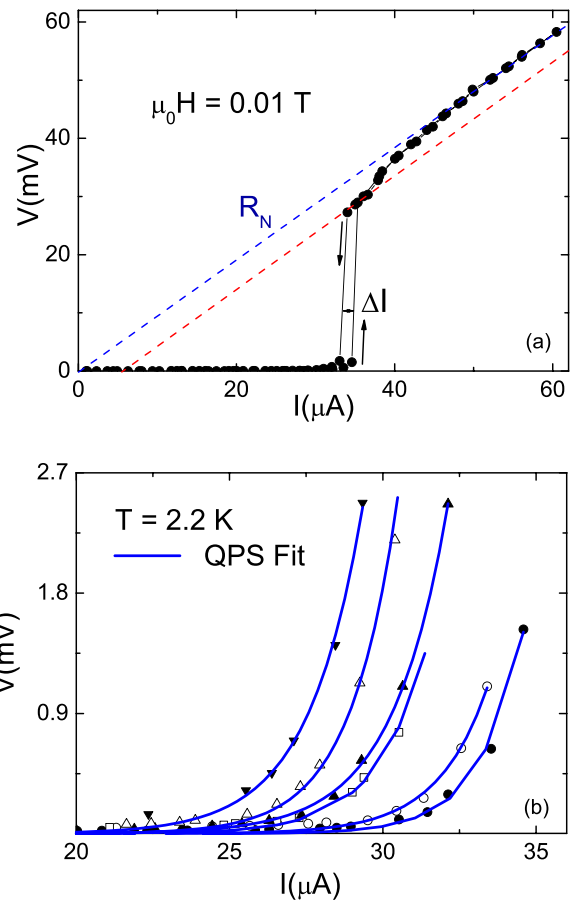$V(I)$ characteristics measured at $T = 2.2$ K for several fields are shown in Fig. 3(b) where, for the sake of legibility,

FIG. 3. (a) $V(I)$ dependence measured at $T = 2.2$ K and $\mu_0 H = 0.01$ T. The red dotted line shows the resistance due to the single phase slip entering the sample. The blue dotted line indicates the normal-state resistance, R_N. (b) Nonlinear voltage versus current characteristics measured at $T = 2.2$ K at different fields. Applied magnetic fields are, from right to left, 0.01, 0.025, 0.05, 0.06, 0.08, and 0.12 T. Blue lines are the QPS fits to the data.

only the curves recorded sweeping the current upward are reported. The curves have been fitted using separately the two exponential expressions valid if TAPS or QPS are responsible for the phase slippage. For thermal activation of phase slips it is[1,17]

$$V_{TAPS} = \frac{2\pi h}{e}\gamma_{TAPS}\sinh\left(\frac{hI}{4ek_BT}\right), \qquad (3)$$

with $\gamma_{TAPS} \sim (R_{TAPS}/R_Q)(k_BT/h)$.[17] If quantum tunneling of phase slips takes place V_{QPS} has a complicated expression which essentially gives for the $V(I)$ dependence a $\sim\sinh(I)$ behavior.[1,10] However, in the high-current (low-temperature) limit, it simply reduces to[1,7,10]

$$V_{QPS} \sim I^{2\mu-1}. \qquad (4)$$

With $\mu = R_Q/R_{qp}$. Here R_{qp} is a resistance of the order of R_N,[7] which can be considered as a fitting parameter. The best fits to the $V(I)$ curves, shown by solid blue lines in Fig. 3(b), were indeed obtained using Eq. (4). The values extracted for the parameter R_{qp} depend on the magnetic field and are all lower than R_N going from $\sim 600 \Omega$ at $\mu_0 H = 0.01$ T to $\sim 800 \Omega$ at $\mu_0 H = 0.14$ T. This result is consistent with the fact that, since R_{qp} represents the low-temperature residual

resistance,[7] it should tend to R_N when the applied magnetic field becomes larger. When the field is further increased beyond 0.14 T the best fit curves do not satisfactorily reproduce the experimental data. Surprisingly, this field is the same at which the hysteresis in the $V(I)$ curves vanishes. We do not have any clear explanation for this coincidence. If, on the other hand, we try to interpret the $V(I)$ characteristics within the model of thermal activation of phase slips, coherently with the results established from the analysis of the $R(T)$ curve, experimental data cannot satisfactorily be fitted if any plausible set of parameters entering γ_{TAPS} is considered in Eq. (3). This result strengthens the idea that current transport properties of the superconducting nanowire network at the chosen (lowest) temperature are mainly due to quantum tunneling of phase slips. Furthermore, it is also worth mentioning that in the case of the $V(I)$ characteristics measured for the wider network[19] it was not possible to fit the curves, in conjunction with the resistive transition, using the same procedure adopted above.

In conclusion, quantum fluctuations of the superconducting order parameter were consistently revealed from both $R(T)$ and $V(I)$ measurements in superconducting Nb nanowire networks patterned on PS templates. The reduction of the number of interconnected wires down to $N \sim 30$ made QPS phenomenon the dominant contribution to the current transport properties of the system. All the data were coherently reproduced in the framework of theoretical models elaborated to describe QPS processes. The analyzed system, obtained starting from a robust and macroscopically large substrate, reveals fascinating quantum effects and shows high values of the critical current density. This last occurrence makes the system of potential use as 1D interconnection in complex nanodevices.[29]

[1]K. Y. Arutyunov, D. S. Golubev, and A. D. Zaikin, Phys. Rep. **464**, 1 (2008).
[2]A. V. Herzog, P. Xiong, F. Sharifi, and R. C. Dynes, Phys. Rev. Lett. **76**, 668 (1996).
[3]D. Y. Vodolazov, F. M. Peeters, L. Piraux, S. Mátéfi-Tempfli, and S. Michotte, Phys. Rev. Lett. **91**, 157001 (2003).
[4]A. Johansson, G. Sambandamurthy, D. Shahar, N. Jacobson, and R. Tenne, Phys. Rev. Lett. **95**, 116805 (2005).
[5]A. Rogachev, A. T. Bollinger, and A. Bezryadin, Phys. Rev. Lett. **94**, 017004 (2005).
[6]M. Tian, J. Wang, J. S. Kurtz, Y. Liu, M. H. W. Chan, T. S. Mayer, and T. E. Mallouk, Phys. Rev. B **71**, 104521 (2005).
[7]M. Zgirski, K. P. Riikonen, V. Touboltsev, and K. Yu. Arutyunov, Phys. Rev. B **77**, 054508 (2008).
[8]F. Altomare, A. M. Chang, M. R. Melloch, Y. Hong, and C. W. Tu, Phys. Rev. Lett **97**, 017001 (2006).
[9]N. Giordano, Phys. Rev. Lett. **61**, 2137 (1988).
[10]A. D. Zaikin, D. S. Golubev, A. van Otterlo, and G. T. Zimányi, Phys. Rev. Lett. **78**, 1552 (1997).
[11]D. S. Golubev and A. D. Zaikin, Phys. Rev. B **64**, 014504 (2001).
[12]C. N. Lau, N. Markovic, M. Bockrath, A. Bezryadin, and M. Tinkham, Phys. Rev. Lett. **87**, 217003 (2001).
[13]D. Pekker, A. Bezryadin, D. S. Hopkins, and P. M. Goldbart, Phys. Rev. B **72**, 104517 (2005).
[14]J. Ku, V. Manucharyan, and A. Bezryadin, Phys. Rev. B **82**, 134518 (2010).
[15]O. V. Astafiev, L. B. Ioffe, S. Kafanov, Yu. A. Pashkin, K. Yu. Arutyunov, D. Shahar, O. Cohen, and J. S. Tsai, Nature **484**, 355 (2012).
[16]U. Patel, Z. L. Xiao, A. Gurevich, S. Avci, J. Hua, R. Divan, U. Welp, and W. K. Kwok, Phys. Rev. B **80**, 012504 (2009).
[17]D. S. Golubev and A. D. Zaikin, Phys. Rev. B **78**, 144502 (2008).
[18]M. Zgirski, K. P. Riikonen, V. Touboltsev, and K. Yu. Arutyunov, Nano Lett. **5**, 1029 (2005).
[19]C. Cirillo, M. Trezza, F. Chiarella, A. Vecchione, V. P. Bondarenko, S. L. Prischepa, and C. Attanasio, Appl. Phys. Lett. **101**, 172601 (2012).
[20]M. Trezza, S. L. Prischepa, C. Cirillo, R. Fittipaldi, M. Sarno, D. Sannino, P. Ciambelli, M. B. S. Hesselberth, S. K. Lazarouk, A. V. Dolbik, V. E. Borisenko, and C. Attanasio, J. Appl. Phys. **104**, 083917 (2008).
[21]M. Trezza, C. Cirillo, S. L. Prischepa, and C. Attanasio, Europhys. Lett. **88**, 57006 (2009).
[22]J. S. Lehtinen, T. Sajavaara, K. Yu. Arutyunov, M. Yu. Presnjakov, and A. L. Vasiliev, Phys. Rev. B. **85**, 094508 (2012).
[23]M.-H. Bae, R. C. Dinsmore III, T. Aref, M. Brenner, and A. Bezryadin, Nano Lett. **9**, 1889 (2009).
[24]P. Xiong, A. V. Herzog, and R. C. Dynes, Phys. Rev. Lett. **78**, 927 (1997).
[25]H. S. J. van der Zant, M. N. Webster, J. Romijn, and J. E. Mooij, Phys. Rev. B. **50**, 340 (1994).
[26]M. Y. Kupriyanov and V. F. Lukichev, Fiz. Nizk. Temp. **6**, 445 (1980) [Sov. J. Low Temp. Phys. **6**, 210 (1980)].
[27]P. Sabatino, C. Cirillo, G. Carapella, M. Trezza, and C. Attanasio, J. Appl. Phys. **108**, 053906 (2010).
[28]A. Rogachev and A. Bezryadin, Appl. Phys. Lett. **83**, 512 (2003).
[29]Y. S. Hor, U. Welp, Y. Ito, Z. L. Xiao, U. Patel, J. F. Mitchell, W. K. Kwok, and G. W. Crabtree, Appl. Phys. Lett. **87**, 142506 (2005).